WILEY

Water transport and tracer mixing in volcanic ash soils at a tropical hillslope: A wet layered sloping sponge

Giovanny M. Mosquera[1,2] [ID] | Patricio Crespo[1] | Lutz Breuer[2,3] | Jan Feyen[1] | David Windhorst[2]

[1]Departamento de Recursos Hídricos y Ciencias Ambientales, Facultad de Ingeniería & Facultad de Ciencias Agropecuarias, Universidad de Cuenca, Cuenca, Ecuador

[2]Institute for Landscape Ecology and Resources Management (ILR), Research Centre for BioSystems, Land Use and Nutrition (iFZ), Justus Liebig University, Giessen, Germany

[3]Centre for International Development and Environmental Research (ZEU), Justus Liebig University, Giessen, Germany

Correspondence
Giovanny M. Mosquera, Departamento de Recursos Hídricos y Ciencias Ambientales, Facultad de Ingeniería & Facultad de Ciencias Agropecuarias, Universidad de Cuenca, Av. 12 de Abril, Cuenca, Ecuador.
Email: giovamosquera@gmail.com, giovanny.moquerar@ucuenca.edu.ec

Funding information
Deutsche Forschungsgemeinschaft, Grant/Award Numbers: BR2238/14-2, BR2238/31-1, WI4995/2-1; Dirección de Investigación de la Universidad de Cuenca (DIUC), Grant/Award Number: PIC-13-ETAPA-001; Secretaría de Educación Superior, Ciencia, Tecnología e Innovación, Grant/Award Number: PIC-13-ETAPA-001

Abstract

Andosol soils formed in volcanic ash provide key hydrological services in montane environments. To unravel the subsurface water transport and tracer mixing in these soils we conducted a detailed characterization of soil properties and analyzed a 3-year data set of sub-hourly hydrometric and weekly stable isotope data collected at three locations along a steep hillslope. A weakly developed (52–61 cm depth), highly organic andic (Ah) horizon overlaying a mineral (C) horizon was identified, both showing relatively similar properties and subsurface flow dynamics along the hillslope. Soil moisture observations in the Ah horizon showed a fast responding (few hours) "rooted" layer to a depth of 15 cm, overlying a "perched" layer that remained near saturated year-round. The formation of the latter results from the high organic matter (33–42%) and clay (29–31%) content of the Ah horizon and an abrupt hydraulic conductivity reduction in this layer with respect to the rooted layer above. Isotopic signatures revealed that water resides within this soil horizon for short periods, both at the rooted (2 weeks) and perched (4 weeks) layer. A fast soil moisture reaction during rainfall events was also observed in the C horizon, with response times similar to those in the rooted layer. These results indicate that despite the perched layer, which helps sustain the water storage of the soil, a fast vertical mobilization of water through the entire soil profile occurs during rainfall events. The latter being the result of the fast transmissivity of hydraulic potentials through the porous matrix of the Andosols, as evidenced by the exponential shape of the water retention curves of the subsequent horizons. These findings demonstrate that the hydrological behavior of volcanic ash soils resembles that of a "layered sponge," in which vertical flow paths dominate.

KEYWORDS

Andosol/andisol, hillslope hydrology, soil moisture, stable isotopes, subsurface flow path, transit time, tropical alpine (Páramo), vadose/unsaturated zone

---

1 | INTRODUCTION

Hillslope soils in mountainous environments are essential providers of hydrological services. They regulate the transport and mixing of water and solutes in the subsurface (Fan et al., 2019; Lin, 2010). Most of these soils are able to store large amounts of water in their matrix (e.g., organic rich soils; van Huijgevoort, Tetzlaff, Sutanudjaja, & Soulsby, 2016; Lazo, Mosquera, McDonnell, & Crespo, 2019) or to deliver it rapidly to streams via preferential and/or shallow subsurface flow (e.g., steep and forested catchments; Anderson, Weiler, Alila, & Hudson, 2009; McDonnell, Owens, & Stewart, 1991; Uchida, Kosugi, & Mizuyama, 1999). The hydrological behavior of mountain soils depends on their specific physical, and chemical properties (e.g., hydraulic conductivity, bulk density [BD], porosity, organic matter content, texture). Despite the importance of hillslope soils in the provisioning of hydrological services, fundamental knowledge about how their properties influence water transport and mixing in the subsurface is lacking (Fan et al., 2019).

Filling this knowledge gap is of particular importance in understudied hydrological systems, such as those in which subsurface flow paths are influenced by the presence of soils of volcanic ash origin. These soils are known as Andosols (IUSS Working Group WRB, 2015) or Andisols (Soil Survey Staff, 1999). Andosols are characterized by their high content of short-range order clays with high surface areas (e.g., allophane, imogolite, ferrihydrite, and/or the Al- and Fe-humus complexes) and organic matter (McDaniel, Lowe, Arnalds, & Ping, 2012), resulting in high water holding capacity (Neall, 2006). These soils occur extensively in mountainous regions around the world with active or recently extinct volcanos (Takahashi & Shoji, 2002) and deliver important hydrological services such as water storage and flow regulation for downstream water users. Therefore, knowledge about how hillslopes underlain by Andosols store and release water is crucial to improve the management of water and soil resources in these regions. However, the understanding of how these soils and their properties influence subsurface hydrological behavior has not yet been sufficiently clarified.

One of the main factors behind this knowledge gap is the lack of data sets that allows full disentanglement of water flow and mixing processes in the subsurface (Vereecken et al., 2015). The use of hydrometric information (e.g., soil moisture and/or matric potential data) has been helpful to identify, for example, (a) spatial and/or temporal dynamics of soil moisture (Blume, Zehe, & Bronstert, 2009; Hasegawa & Eguchi, 2002), (b) hydrometeorological controls on soil moisture response during rainfall events (Tenelanda-Patiño, Crespo-Sánchez, & Mosquera-Rojas, 2018), (c) subsurface flow processes (Eguchi & Hasegawa, 2008; Hasegawa & Sakayori, 2000), and (d) the effects of land use and/or land cover change in soil moisture dynamics (Dec et al., 2017; Montenegro-Díaz, Ochoa-Sánchez, & Célleri, 2019) in plots and hillslopes underlain by Andosols. Nevertheless, hydrometric observations alone are insufficient to shed light on water mixing and aging within these soils.

In the last two decades, insights into subsurface mixing processes and water ages improved thanks to the monitoring of the stable isotopes of hydrogen and oxygen (^2H and ^{18}O) in soil waters (Sprenger, Leistert, Gimbel, & Weiler, 2016). Tracer data do not only allow to investigate how incoming precipitation mixes with water previously stored in the soils, but also for the estimation of the "age" or mean transit time (MTT; i.e., the time it takes for a water molecule to travel to the outlet of a hydrological system; McGuire & McDonnell, 2006) of water mobilizing within different soil layers/horizons (Asano, Uchida, & Ohte, 2002; Lazo et al., 2019; McGuire & McDonnell, 2010; Muñoz-Villers & McDonnell, 2012; Stumpp, Maloszewski, Stichler, & Fank, 2009; Tetzlaff, Birkel, Dick, Geris, & Soulsby, 2014). Soil water MTT evaluations at hillslope transects have shown either a dominance of water aging with depth below the surface (Asano et al., 2002; McGuire & McDonnell, 2010; Muñoz-Villers & McDonnell, 2012) or a combination of depth and upslope contributing area (Kim & Jung, 2014; Stewart & McDonnell, 1991; Tetzlaff et al., 2014). The former indicates that vertical flow paths are dominant, and the latter that there is also a significant influence of lateral subsurface flow paths. Although soil water isotopes (SWIs) in Andosols have been used to investigate runoff generation (Mosquera et al., 2016; Muñoz-Villers & McDonnell, 2012) and water storage (Lazo et al., 2019) in catchments, their application in combination with hydrometric observations and detailed characterization of soil properties is still inexistent. This situation hinders our ability to disentangle flow paths and mixing processes in hillslopes dominated by volcanic ash soils.

To fill this knowledge gap, we present a unique data set of soil properties in combination with hydrometric and water isotope measurements in precipitation and soil water collected in an experimental hillslope transect underlain by volcanic ash soils (Andosols). The experimental hillslope is located within the tropical alpine (Páramo) ecosystem in south Ecuador. This rich set of observations was analyzed to address the following overarching question: how does water transport and mix in volcanic ash soils (Andosols) at the hillslope scale? To this end, the two objectives of this research are: (a) to evaluate how Andosols' properties influence water flow and mixing in the subsurface, and (b) to conceptualize the subsurface hydrological behavior and the dominant flow paths of water occurring within the experimental hillslope.

2 | EXPERIMENTAL HILLSLOPE DESCRIPTION

The study was carried out at a tropical alpine (Páramo) experimental hillslope situated in the headwaters of the Quinuas Ecohydrological Observatory in south Ecuador (2°47′S, 79°13′W) between 3,900 and 4,100 m a.s.l. The hillslope (Figure 1a) has a steep gradient (42%; similar to the average slope of the Quinuas Observatory; Pesántez, Mosquera, Crespo, Breuer, & Windhorst, 2018) and is covered by the dominant Páramo vegetation, consisting primarily of tussock grass (*Calamagrostis intermedia*), locally known as "pajonal," which covers more than 75–80% of conserved Páramo areas (Mosquera, Lazo, Célleri, Wilcox, & Crespo, 2015). The soils at the study region resulted from the accumulation of volcanic ash deposits during Quaternary
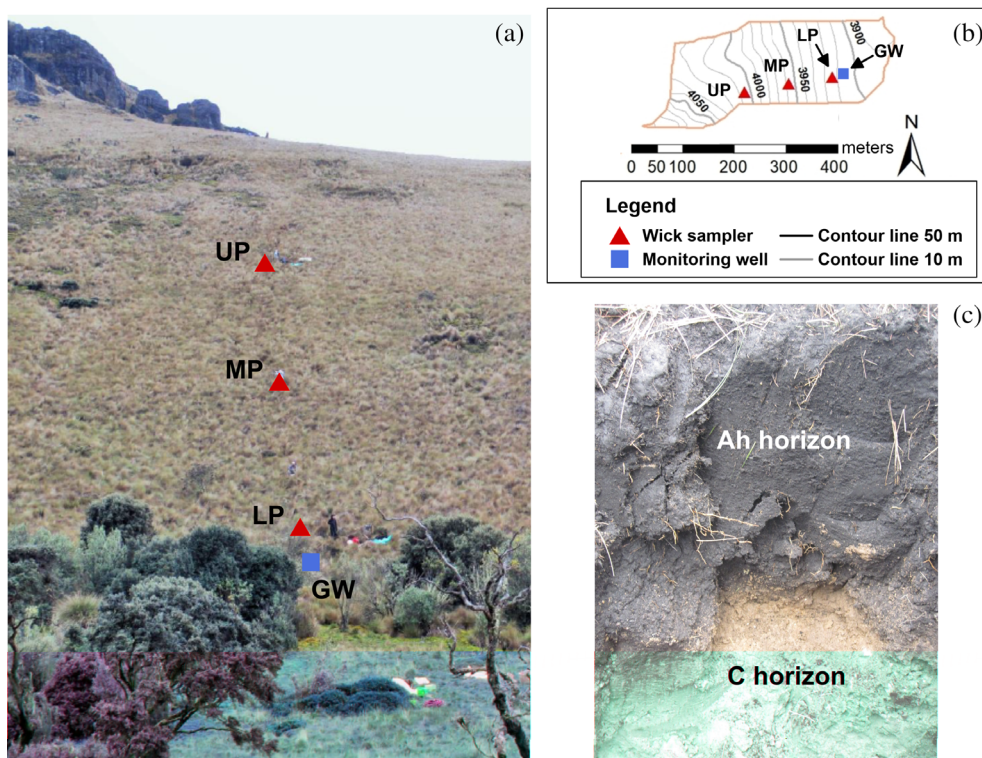
FIGURE 1 (a) Experimental hillslope showing the monitoring stations of soil moisture content and stable isotopes of soil water at the upper (UP), middle (MP), and lower (LP) positions (red triangles) along the experimental hillslope and the position of a monitoring well used for monitoring the groundwater level at the bottom of the hillslope (GW, blue square); (b) hillslope drainage area and monitoring stations; and (c) soil profile and horizons at the UP of the hillslope. Ah = Andic horizon, C = mineral horizon

activity in combination with the humid and cold local climate conditions (Buytaert et al., 2006). These conditions have led to the formation of organic and clay rich soils with high water holding capacity (i.e., Andosols). The soils in the study region are characterized as nonallophanic (i.e., the clay mineralogy is dominated by metal-humus complexes; Buytaert, Deckers, & Wyseure, 2006). The climate is mainly influenced by continental air masses originating from the Amazon basin (Esquivel-Hernández et al., 2019). Precipitation occurs throughout the year and is composed mainly of drizzle (Padrón, Wilcox, Crespo, & Célleri, 2015). Annual precipitation during the period 2015–2018 averages 1,021 mm, with low temporal seasonality (Carrillo-Rojas, Silva, Rollenbeck, Célleri, & Bendix, 2019; Muñoz, Orellana-Alvear, Willems, & Célleri, 2018). Average temperature and average relative humidity during the period 2011–2014 are 5.4°C and 92.1% at 3,955 m a.s.l., respectively (Muñoz, Célleri, & Feyen, 2016).

3 | DATA COLLECTION AND METHODS

3.1 | Soil properties characterization

Soil pits were dug to characterize the soil profile at three locations along the experimental hillslope. The upper position (UP) at 4,006 m a.s.l., the middle position (MP) at 3,958 m a.s.l., and the lower position (LP) at 3,913 m a.s.l (Figure 1a,b). The length between the UP and LP sampling sites was 208 m. The UP site was located 256 m below the hilltop. The type, depth, and density of roots in each soil horizon (including the densely rooted topsoil layer) were determined according to the FAO guidelines (FAO, 2006). The distribution of coarse and fine particles and the field characterization of soil texture

were carried out according to ISO 11277:2009 International Standard (ISO 11277, 2009). Soil carbon content (CC) was determined via combustion of two undisturbed soil samples collected at each sampling position and depth using a Vario EL cube device (Elementar, Germany). CC was used as an indicator of soil organic matter content (OM% = CC% × 1.72; Guo & Gifford, 2002).

The hydraulic properties of the soils were also characterized at 5, 20, 45, and 75 cm depths at the same positions as the soil pits. The saturated hydraulic conductivity (k_{sat}) of the soils in the vertical direction was measured in situ via the inverse auger-hole method (Oosterbaan & Nijland, 1994). The measurements were repeated three times at each position and depth, and the average k_{sat} values are reported. Three undisturbed soil samples were collected using 100 cm^3 steel rings to determine BD and soil moisture content at saturation. The latter was determined gravimetrically as the weight difference of the samples saturated via capillary rise and subsequently oven-dried at 105°C for 24 hr. The BD and soil moisture at saturation values are reported as average values for the three replicates.

The moisture release curves of the organic and mineral horizons of the soils were also determined. Given the highly organic nature of the shallow horizon of the hillslope soils, their moisture release curves were determined from direct soil moisture content and matric potential measurements (Vereecken et al., 2008) using time domain reflectometers (Campbell Scientific CS616) and tensiometers (UMS T8), respectively. For this purpose, we took three randomly selected undisturbed soil cores (Ø = 40 cm, h = 32 cm) located in a 5 m × 5 m area around each of the sampling sites along the hillslope to capture the spatial variability of the moisture release characteristic. The samples were wetted from the bottom of the cores via capillary rise for 2 months to assure they

were completely saturated. Once the samples were fully saturated, we installed one reflectometer and one tensiometer at a depth of 15 cm below the vegetation layer in each soil core. The samples were then drained freely by gravity and their soil moisture content-water potential relations were measured at 5-min intervals until the tensiometer probes lost contact with the matrix due to desiccation.

The stoniness of the mineral horizon of the soils did not allow collecting large undisturbed soil cores to determine moisture release characteristics as described above. Thus, the soil moisture-matric potential relations were determined using 100 cm^3 undisturbed soil samples by applying traditional laboratory analyses using sandboxes (Topp & Zebchuk, 1979) and pressure chambers (FAO, 2002). Soil moisture was determined at matric potentials of 1, 3, 10, 31, 330, 2,500, and 15,000 cm H_2O, which span a range from saturation (1 cm H_2O) to theoretical permanent wilting point (~15,000 cm H_2O). Given the similarities among the water retention curves collected at each soil horizon along the hillslope, we report these results as the average ± 1 SD of all analyzed samples.

3.2 | Hydrometric data collection

The hillslope was equipped for the monitoring of hydrometric fluxes (rainfall, soil moisture, and groundwater level) and tracer fingerprints (SWI) at the same three positions as the soil pits. A Texas TE525MM tipping bucket rain gauge with an accuracy of ±1% was used to record precipitation amounts 1.5 km from the experimental hillslope at an elevation of 3,955 m a.s.l. Soil moisture content was measured using Decagon Devices 5TE capacitance probes. The capacitance probes were installed at the UP, MP, and LP sampling sites (Figure 1a,b) at 5, 20, 45, and 75 cm depths. The probes were calibrated for the soils' local conditions for each of the identified horizons following the procedures described by Blume et al. (2009). Through calibration, an improved accuracy of ±1–2% (r^2 = .95, p-value <.05) was obtained (Tenelanda-Patiño et al., 2018). Rainfall amount and soil moisture content data were simultaneously monitored every 5-min during the period January 2015–December 2017.

We also used a monitoring well to measure groundwater level fluctuations at the bottom of the experimental hillslope (GW site in Figure 1a,b). The well consisted of 1.5 m long, 2-in. (5.1 cm) diameter galvanized tube, with a 1.05 m screen with holes of 0.8 mm diameter separated 10 mm vertically and 5 mm horizontally. Given the highly organic nature of the local soils, we designed a filter system following the recommendations of the Minnesota Board of Water & Soil Resources for hydrologic monitoring of wetlands (Minnesota Board of Water & Soil Resources, 2013). The well was wrapped with a permeable nylon textile and a 5 cm sand and gravel filter (1–20 mm diameter) to prevent sediment accumulation in the tube. Approximately 70% of the filter was composed of fine sand particles (1 mm diameter) to increase the surface area where organic matter particles could be retained. Pressure transducers (Schlumberger DI500) with a precision of ±5 mm recorded groundwater level fluctuations every 5-min during the period January–December 2017.

3.3 | Isotopic data collection and analysis

Precipitation water samples were collected from a rainfall collector installed at the location of the rain gauge. The rainfall collector was covered with aluminum foil and a 5 mm mineral oil layer was added to the collector to reduce possible isotopic fractionation due to evaporation. A portion of the mobile water fraction of the soils was collected using wick samplers (Mertens & Vanderborght, 2007). The wick samplers consisted of a 30 cm × 30 cm polypropylene plate surrounded by 5 cm walls, on which a piece of 0.5 m long woven and braided 3/8″ fiberglass wick (Amatex Co., Norristown, PA) was unraveled and covered with parent soil material. Below the polypropylene plates, the remaining part of the wicks were placed inside a flexible silicon tube and protected with a 60 cm long and 3/4″ diameter plastic pipe to ensure an unhindered and constant vertical suction of approximately 60 hPa (Windhorst, Kraft, Timbe, Frede, & Breuer, 2014). Each silicon tube was routed to a centralized collection pipe (Ø = 50 cm) where it was connected to a 1.5-L glass bottle where collected water was stored until analysis (Pesántez et al., 2018). The wick samplers were installed at 10, 35, and 65 cm depths at each sampling site.

The precipitation and soil water samples were collected weekly for the period January–December 2016. The collected samples were filtered in the field using 0.45 μm polytetrafluoroethylene membranes and stored in 2-mL amber glass bottles in the dark to prevent evaporative fractionation until analysis (Mook, 2000). The samples were analyzed for ^2H and ^{18}O using a Picarro L2130-i isotopic water vapor analyzer with a precision of 0.5‰ for ^2H and 0.2‰ for ^{18}O. The ChemCorrect software (Picarro, 2010) was used to check the samples for organic contamination. Samples that showed evidence of contamination were excluded from data analysis. The isotopic values are reported in the δ notation in reference to the Vienna Standard Mean Ocean Water V-SMOW for both measured isotopes (Craig, 1961).

3.4 | Spatiotemporal variability of hydrometric data: Hydrological dynamics and response times

The transport of water in the subsurface was characterized through the temporal variability of hydrometric observations and the response time of soil moisture and groundwater level to rainstorm events. We first plotted and compared hourly data of precipitation, soil moisture content, and groundwater level, and carried out an examination of the response times to reach the peak value (t_{peak}) of soil moisture or groundwater level during rainstorm events (Zhu, Nie, Zhou, Liao, & Li, 2014). Rainfall events were defined using the minimum inter-event time criteria (Dunkerley, 2008). That is, the minimum time span without rain between two consecutive events. Given that precipitation occurs frequently in the study region, with only few consecutive dry days throughout the year (Padrón et al., 2015), a time-lapse of 6 hr without rain was used to characterize rainfall events (Tenelanda-Patiño et al., 2018). The manufacturers' accuracy of the instruments, 0.3% volume for soil moisture and 0.5 cm H_2O for groundwater level, was applied as minimum threshold changes to differentiate instruments noise from

response to rainfall during the events (Lozano-Parra, Van Schaik, Schnabel, & Gómez-gutiérrez, 2015). Only events in which data were available at all sampling locations were considered. Under these conditions, 74 rainfall events were identified. The t_{peak} information was used to compare the timing of soil moisture response along the experimental hillslope. For this purpose, scatter plots of t_{peak} between pairs of contiguous sampling positions at the same sampling depth (e.g., between the UP and MP at 5 cm depth) and contiguous sampling depths at the same sampling position (e.g., between 20 and 45 cm depths at the MP) were constructed and analyzed. The same approach was carried out to compare the t_{peak} between soil moisture at different depths at the LP site and the groundwater levels at the bottom of the hillslope. In these analyses, scatter points falling closely to the 1:1 ratio indicate similar response times, whereas the ones falling outside this relation indicate delays in response time between different sampling positions/depths or groundwater levels.

3.5 | Soil water stable isotopes: Tracer mixing and soil water ages

The mixing of tracer in the system was evaluated via the attenuation of the isotopic composition of soil water (at different positions and depths) in relation to the composition of precipitation. For this purpose, we compared the weekly collected stable isotopic composition of rainfall and soil water samples. This analysis permitted a qualitative characterization of how the water within the soils mixes with rainfall water. In addition, we used δ^2H–$\delta^{18}O$ isotope plots of precipitation samples (i.e., the local meteoric water line, LMWL; Rozanski et al., 1993) and soil waters to evaluate potential evaporation effects in the isotopic fractionation of soil water (i.e., nonequilibrium fractionation).

We applied a lumped convolution approach (LCA; Maloszewski & Zuber, 1996) to estimate the MTT (age) of soil water. The LCA approach aims to reproduce the attenuation of the geochemical composition of a given tracer (e.g., ^2H, ^{18}O, Cl) at the outlet of a hydrologic system based on the tracer's input signal assuming steady state conditions. Even though alternative methods for the investigation of water ages under nonstationary conditions exist (Benettin et al., 2017; Harman, 2015; Kirchner, 2016), since our objective is not to investigate long-term changes in subsurface hydrological conditions, the LCA provides a valuable metric that allows for a quantitative comparison of the attenuation of the isotopic composition of soil water at different sampling positions and depths. Since it can be assumed that our experimental hillslope is subjected to the same meteorological conditions along the whole monitoring transect, such a comparison permits to identify the dominant flow paths of water in the subsurface.

Transit time distributions (TTDs) are used in the LCA to convert inputs tracer signals into output ones. TTDs are predefined mathematical functions that represent the internal transport and mixing processes within hydrologic systems (Hrachowitz et al., 2016). We applied the exponential model (EM) TTD as it has outperformed at catchment (Mosquera et al., 2016; Muñoz-Villers, Geissert, Holwerda, & Mcdonnell, 2016) and hillslope (Lazo et al., 2019; Muñoz-Villers & McDonnell, 2012)

scales in the Páramo and other tropical montane ecosystems in comparison to other TTDs. The model performance was evaluated using the Kling–Gupta efficiency (KGE; Gupta, Kling, Yilmaz, & Martinez, 2009). The model was run 10,000 times using a Monte Carlo sampling procedure to calibrate the only parameter of the EM TTD, that is, the MTT of the system. The range of calibration parameters was 0–250 weeks (0–5 years). Simulations that yielded at least 95% of the highest KGE were considered behavioral solutions. The 5 and 95% bounds of the range of behavioral solution parameters were used as uncertainty limits for the model simulations. Further details about the modeling procedure can be found in Mosquera, Segura, et al. (2016).

4 | RESULTS

4.1 | Soil properties characterization

The general characteristics of the soil profiles along the experimental hillslope are shown in Table 1. These were generally consistent with those reported for nearby Páramo hillslopes (Buytaert, Deckers, & Wyseure, 2006; Mosquera, Célleri, et al., 2016) and in a tropical forest catchment dominated by Andosol soils in central eastern Mexico (Muñoz-Villers & McDonnell, 2012). There were two well-differentiated soil horizons (Figure 1c). The shallow horizon corresponded to an andic horizon (Ah) with relatively comparable characteristics at all sampling sites. Its depth varied little (52–61 cm) along the hillslope. The Ah horizon contained a high density of fine roots (Ø ≤ 2 mm), with the highest density in the first 10–15 cm below the ground surface due to the presence of the root system of the overlying tussock grass vegetation. The density of large roots (Ø > 2 mm) was lower than the density of fine roots. In this horizon few coarse particles, most of them with Ø ≤ 200 mm, were present. Its texture was classified as clay loam. The distribution of fine particles in the Ah horizon was similar at all sampling sites (sand 29–39%, silt 32–42%, and clay 29–31%). The CC in the Ah horizon was high at all hillslope positions (19.5–24.5%, corresponding to organic matter contents of 33.5–42.1%).

The underlying horizon corresponded to a mineral horizon (C) with more heterogeneous characteristics. The depth of the C horizon was higher at the LP site compared to the UP and MP sites. The density of fine roots was very low and there were no large roots. The proportion of coarse particles was higher than for the Ah horizon. The majority of particles (48–57% of the total) had Ø > 200 mm, regardless of the position along the hillslope. The texture of the C horizon was classified as sandy loam. The distribution of fine particles revealed a dominance of sand (70–73%) and low clay content (7–8%). The CC was much lower than in the Ah horizon and decreased with sampling site elevation from 4.4% at the UP site to 1.7% at the LP site.

The hydraulic properties of the soils along the experimental hillslope are summarized in Table 2. The BD of the Ah horizon was relatively similar at all depths (5, 20, and 45 cm) at each sampling position, with typically low values (<0.90 g cm^{-3}) expected for the Ah horizon of Andosol soils (Takahashi & Shoji, 2002). The BD varied between 0.37 ± 0.07 g cm^{-3} and was least variable with depth at the UP site.

TABLE 1 Physical characteristics and carbon content of the soil profiles monitored at the upper (UP), middle (MP), and lower (LP) positions along the experimental hillslope

Hillslope position	Altitude (m a.s.l.)	Horizon type	Upper boundary (cm)	Lower boundary (cm)	Root content Fine [Ø ≤ 2 mm] (roots per dm²)	Large [Ø > 2 mm] (roots per dm²)	Coarse particles distribution 2–63 mm (%)	63–200 mm (%)	>200 mm (%)	Fine particles distribution[a] Sand (%)	Silt (%)	Clay (%)	Carbon content[b] (%)
UP	4,006	Ah$_{DRZ}$	0	10	224	0	0	0	0	29	42	30	24.4
		Ah$_{BDRZ}$	10	57	63	7	4	2	0				24.5
		C	57	89	4	0	5	8	12	73	20	7	4.4
MP	3,958	Ah$_{DRZ}$	0	10	280	0	0	0	0	34	35	31	33.8
		Ah$_{BDRZ}$	10	52	57	3	4	2	0				19.5
		C	52	77	11	0	10	5	20	71	22	7	2.3
LP	3,913	Ah$_{DRZ}$	0	10	200	0	0	0	0	39	32	29	27.3
		Ah$_{BDRZ}$	10	61	58	9	5	1	1				21.2
		C	61	116	4	0	10	2	12	70	23	8	1.7

Abbreviations: Ah, andic horizon; C, mineral horizon; DRZ, densely rooted zone; BDRZ, below densely rooted zone; Ø, diameter of the roots.
[a]The distribution of fine particles in the andic (Ah) horizon was only characterized at half the depth of the soil horizon at each sampling site.
[b]The soil samples for carbon content analysis were taken at depths corresponding to half the horizon/layer thickness (i.e., the average between the upper and lower boundaries reported in the table).

TABLE 2 Mean values of the hydrophysical properties of the soil at the upper (UP), middle (MP), and lower (LP) positions along the experimental hillslope

| Hillslope position	Altitude (m a.s.l.)	Depth (cm)	Horizon	BD (g cm^{-1})	K_{sat} (cm hr^{-1})	θ_{sat} (cm^3 cm^{-3})
UP	4,006	5	Ah	0.29	1.41	0.84
		20	Ah	0.29	0.45	0.80
		45	Ah	0.30	0.25	0.85
		75	C	1.12	1.12	0.59
MP	3,958	5	Ah	0.37	1.88	0.82
		20	Ah	0.46	0.65	0.78
		45	Ah	0.51	0.31	0.78
		75	C	1.37	2.28	0.48
LP	3,913	5	Ah	0.33	1.91	0.84
		20	Ah	0.39	0.42	0.84
		45	Ah	0.35	0.30	0.84
		75	C	0.96	2.73	0.55

Note: The presented values correspond to the average of three measurements of each of the properties and each sampling location and depth.
Abbreviations: BD, bulk density; K_{sat}, saturated hydraulic conductivity in the vertical direction; θ_{sat}, soil moisture content at saturation.

The BD in the C horizon (75 cm depth) was consistently higher than in the Ah horizon at all sampling sites (0.96–1.37 g cm^{-3}). The K_{sat} of the Ah horizon in the vertical direction generally decreased with depth, with values up to 1.91 cm hr^{-1} at 5 cm depth, and as low as 0.25 cm hr^{-1} at 45 cm depth. The K_{sat} of the C horizon (1.12–2.73 cm hr^{-1}) was higher than for the Ah horizon and was highest downslope. The BD and K_{sat} values for both horizons are consistent with those previously reported along hillslopes in nearby Páramo areas (Buytaert, Deckers, & Wyseure, 2006; Mosquera, Célleri, et al., 2016). The soil moisture content at saturation was high, as expected for soils rich in organic

matter (Boelter, 1969; Letts, Roulet, Comer, Skarupa, & Verseghy, 2000), and similar at all soil depths within the Ah horizon at all sampling positions (0.78–0.84 cm^3 cm^{-3}). The soil moisture content at saturation in the C horizon was substantially lower than in the Ah horizon (Buytaert, Deckers, & Wyseure, 2006), and varied little along the hillslope (0.48–0.59 cm^3 cm^{-3}).

The moisture release curve of the organic horizon of the hillslope soils depicted an exponential decrease in soil moisture as matric potentials increased from saturation to ~330 cm H$_2$O (Figure 2a), resembling the soil moisture retention curve of peat soils (Schwärzel
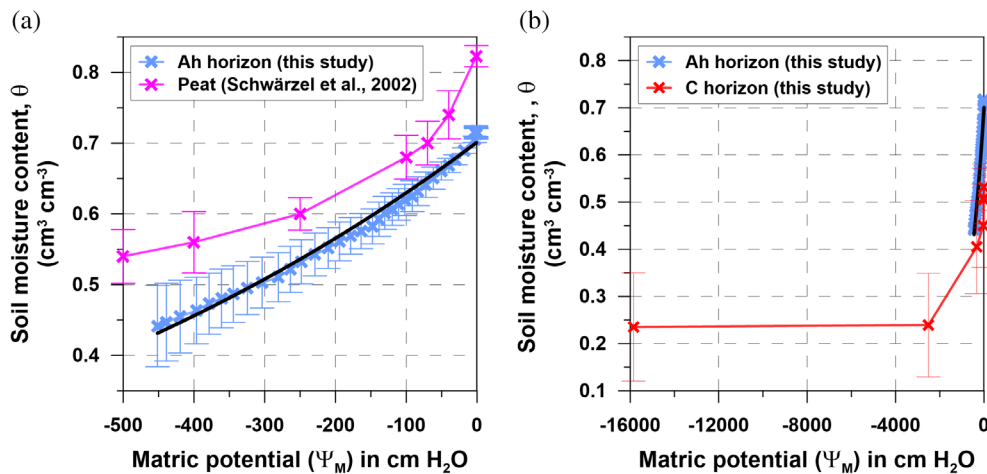
FIGURE 2 Moisture release curves of the (a) organic (Ah) horizon (including the curve for a peat soil reported by Schwärzel, Renger, Sauerbrey, & Wessolek, 2002 for reference) and (b) the mineral (C) horizon (including the curve of the Ah horizon for reference) of the experimental hillslope soils. The black lines in subplots (a) and (b) show the exponential relation between the matric potential and soil moisture content of the Ah horizon (Eq: $\ln [\theta] = 1.076e^{-3} \times \Psi_M - 0.3548$). Note the different ranges of the *x*- and *y*-axes values in subplots (a) and (b). Data shown represent the mean (x symbols) and standard deviation (error bars) of all samples collected at the upper (UP), middle (MP), and lower (LP) sampling sites along the experimental hillslope for each soil horizon

et al., 2002) and those obtained for Andosol soils in the Terceira Island, Portugal (Fontes, Gonçalves, & Pereira, 2004). The water retention curve of the mineral horizon resembled that of the organic horizon at potential values above field capacity, but with lower moisture contents for the same potentials (Figure 2b). This relation further showed a decrease in soil moisture with decreasing potentials to a soil moisture of 0.24 ± 0.11 cm^3 cm^{-3} at permanent wilting point (~15,000 cm H$_2$O).

4.2 | Hydrological dynamics and response times

Hourly rainfall, soil moisture content, and groundwater level data are shown in Figure 3. Precipitation was uniform during the study period and fell typically as low intensity events (<2 mm hr^{-1}), although few rainstorm events had a maximum intensity that exceeded 5 mm hr^{-1} (Figure 3a).

The soil moisture dynamics at 5 cm depth (the densely rooted zone of the Ah horizon; hereafter referred to as the "rooted layer") varied along the hillslope (grey lines in Figure 3b,d). At the UP site, soil moisture varied between 0.46 cm^3 cm^{-3} during periods of low intensity precipitation and saturation (0.84 cm^3 cm^{-3}) in response to high intensity precipitation events (Figure 3b). A similar hydrological dynamic was observed at the MP site, but at higher soil moisture than at the UP site (Figure 3c). Soil moisture at the LP site varied little and remained near saturated (0.84–0.82 cm^3 cm^{-3}, respectively), except during relatively long dry periods (e.g., October–December 2016; Figure 3d).

At 20 cm depth, the soil moisture dynamic at all hillslope positions was very different than in the rooted layer (black lines in Figure 3b,d). That is, there was no apparent soil moisture response to the temporal variability in precipitation. Soil moisture remained high and near saturation (0.72 ± 0.05 cm^3 cm^{-3}) during the entire study period, even during extended dry periods. These conditions resemble

a perched water layer in the Ah horizon, and as such, this layer will hereafter be referred to as the "perched layer." Although soil moisture at 45 cm depth (the Ah horizon layer near the organic-mineral horizons interface; hereafter referred to as the "transition layer") was more responsive to the temporal variability of precipitation (brown lines in Figure 3b,d), it showed a similar behavior as the perched layer. Soil moisture varied little at the UP site during the study period (0.68–0.71 cm^3 cm^{-3}). At the MP site, soil moisture varied between 0.53 cm^3 cm^{-3} during low intensity precipitation periods and was 0.71 cm^3 cm^{-3} during high intensity precipitation events (Figure 3c). Soil moisture at the LP site was higher (>0.72 cm^3 cm^{-3}) than at UP and LP sites during the whole study period, and reached saturation during precipitation events of high intensity (Figure 3d). Regardless of the monitoring position, soil moisture in the transition layer decreased only slightly during dry periods.

The soil moisture dynamics at a depth of 75 cm depth (i.e., within the C horizon), hereafter referred to as the "mineral layer," differed at each of the hillslope positions (orange lines in Figure 3b,d). At the UP site, soil moisture was low and remained below saturation (<0.59 cm^3 cm^{-3}), but was very responsive to precipitation inputs (Figure 3b). At the MP site, soil moisture remained higher in comparison to the UP site and reached saturated conditions (0.48 cm^3 cm^{-3}) during some rainy periods (Figure 3c). Soil moisture was the highest at the LP site and often reached saturation (0.58 cm^3 cm^{-3}; Figure 3d) in comparison to the other hillslope positions. Soil moisture showed only a slight decrease during dry periods at all hillslope positions.

The groundwater level at the bottom of the hillslope responded rapidly to precipitation events, but reached the surface only few times mainly during the wettest months (March–May). Groundwater levels were also more sensitive to relatively long (>1 month) periods of no to low rainfall (Figure 3e). During one of the longest dry periods (August 3–October 5, 2017), groundwater levels steadily decreased to the

FIGURE 3 Hourly temporal variability of (a) precipitation and soil moisture content (θ) at the (b) upper (UP), (c) middle (MP), and (d) lower (LP) positions along the experimental hillslope, and (e) groundwater level (GW) at the bottom of the experimental hillslope located in the headwaters of the Quinuas River Ecohydrological Observatory for the period January 2015–December 2017
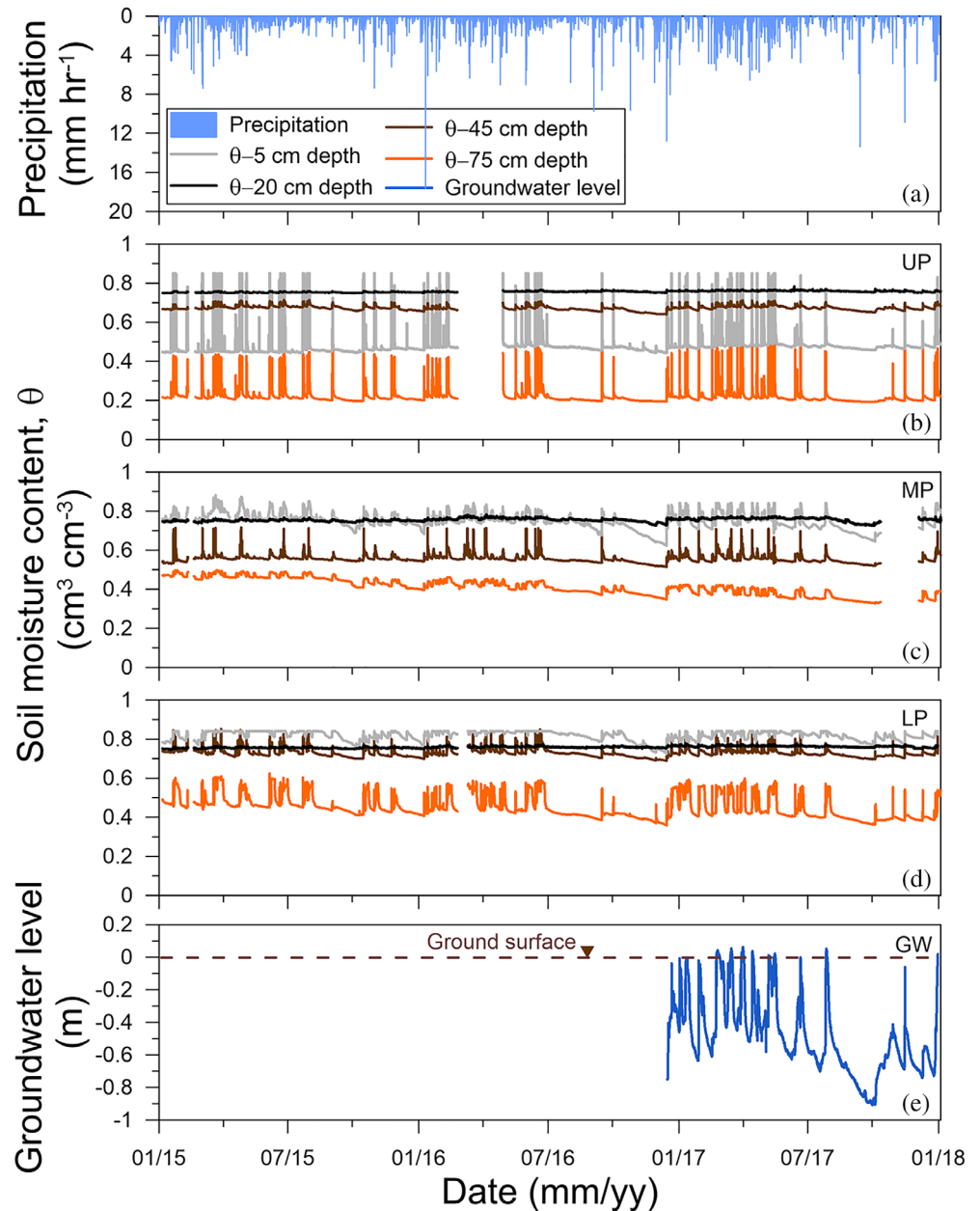

lowest level recorded during the monitoring period (i.e., 97 cm below the ground level) and changed at a faster rate than the soil moisture levels uphill (Figure 3b,d).

The response times to the peak values of soil moisture and groundwater level during precipitation events varied between 1 and 35 hr along the hillslope (Figures 4 and 5). These times were normally short, with an average variation of 7.2 ± 1.6 hr among all sampling sites. The response times at contiguous sampling positions and depths were very similar and fell mostly under the 1:1 relation (Figure 4 and 5c–h). The only exception was in the rooted layer, where we observed a short delay in soil moisture response at the MP site in comparison to the UP site (Figure 5a). We could not evaluate the response times at the LP site in the rooted layer as the soil usually became saturated before the other sampling positions/depths reached maximum soil moisture/groundwater level (Figures 4g and 5b).

4.3 | Tracer mixing and soil water ages

The temporal variability of the isotopic composition of precipitation and soil water is shown in Figure 6. The isotopic composition of soil water in the rooted and perched layers (at 10 and 35 cm depths, respectively; gray and black dots in Figure 6) followed closely the isotopic composition of precipitation. Conversely, the isotopic composition of soil water in the mineral layer (at 65 cm depth; orange dots in Figure 6) was more attenuated than the isotopic compositions of precipitation and soil water in the Ah horizon. The dual plots of $\delta^{18}O$ and $\delta^{2}H$ showed that regardless of the horizon type (i.e., organic or mineral), all soil water samples at all sampling sites plotted within the range of variation of the samples in precipitation (Figure 6b,d,f). These observations indicate that evaporative fractionation of soil water is negligible. Although transpiration does not usually modify the stable
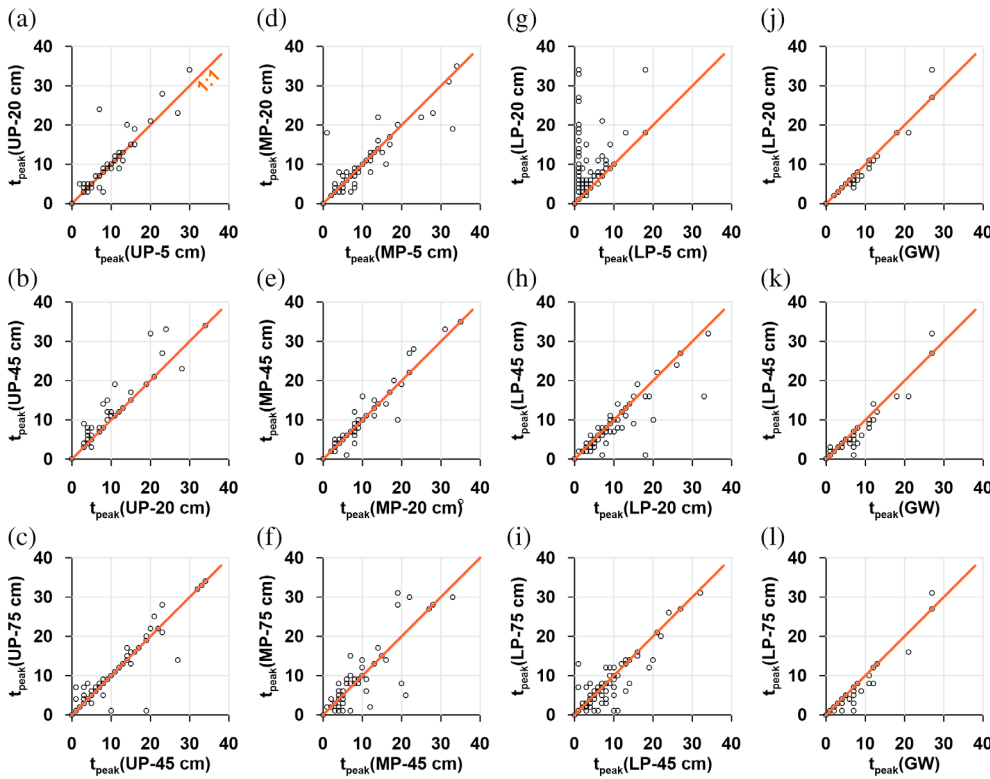
FIGURE 4 Relation of the response times in hours (t_{peak}) to the peak value of soil moisture during rainfall events between contiguous sampling depths at the UP (a–c), MP (d–f), and LP (g–i) sites. Subplots (j)–(l) show the relation between the t_{peak} to the peak value of soil moisture at different depths at the LP site and the t_{peak} to the peak value of groundwater level (GW) at the bottom of the hillslope during rainfall events (j–l). The orange line in each subplot represents the 1:1 ratio

isotopic composition of water (White, 1989), it could affect soil water MTT estimations by removing important amounts of water from the soil. Transpiration of the tussock grass vegetation that covers the experimental hillslope only affects the rooted layer of the soil profile (up to 10–15 cm depth). However, this water flux represents only a small fraction of evapotranspiration in the study region (Ochoa-Sánchez, Crespo, Carrillo-Rojas, Marín, & Célleri, 2020). Evaporation and transpiration effects on the isotopic composition of soil water are likely suppressed by the local environmental conditions. That is, high relative humidity (annual average = 90%; Muñoz et al., 2016), low net radiation (annual average = 100 W m^{-2}; Ochoa-Sánchez et al., 2020), and sustained input of low intensity precipitation (Padrón et al., 2015) throughout the year. Thus, the soil water MTT estimations were unaffected by evaporation and transpiration effects. Soil water MTTs increased consistently from the rooted layer to the mineral layer at all hillslope positions (Figure 7 and Table 3). MTTs varied little at all monitored positions in the rooted (14.3 ± 6.1 days) and perched (26.3 ± 7.4 days) layers within the Ah horizon. On the contrary, there was a larger MTT variation in the mineral layer (from 256.7 ± 34.3 days at the UP to 83.8 ± 13.4 days at the LP; Table 3).

5 | DISCUSSION

5.1 | Hydrological dynamics and response times

Hydrometric observations showed higher moisture contents toward the bottom of the hillslope (Figure 3b–d). This effect likely results

from an increase in the contributing drainage area toward the bottom of the hillslope, possibly combined with a decrease in slope gradient for the sampling sites closer to the valley bottom. These factors probably explain the larger changes in soil moisture contents to occur at the UP site, as soil layers at this position (particularly the rooted and mineral layers) remain drier than those at the MP and LP sites where saturated conditions occurred more frequently. Apart from this difference, soil moisture dynamics was relatively similar at each soil layer along the experimental hillslope.

The rapid response of soil moisture to precipitation inputs in the rooted layer of the Ah horizon (from the ground surface to 10–15 cm depth; Table 1 and gray lines in Figure 3b–d) indicates that this soil layer was highly influenced by the temporal dynamics of incoming precipitation. The fast hydraulic response can be explained by the combination of two factors. First, the activation of preferential flow paths through the layer's large density of roots, as has been previously observed in Japanese Andosol soils (Eguchi & Hasegawa, 2008). This rapid response can be further explained by the fast mobilization of water via matric flow through the porous soil matrix (Hasegawa & Sakayori, 2000; Neall, 2006). A similar hydrological behavior in the unsaturated zone of an organic rich soil layer was observed in a steep hillslope in Coos Bay, OR (Torres, Dietrich, Montgomery, Anderson, & Loague, 1998). There, the observed subsurface flow dynamics were explained by the shape of the soils' water retention curves, which suggested that small changes in hydraulic potentials caused large changes in soil moisture at low matric potentials. The exponentially shaped moisture release curve of the organic horizon of the soils in the experimental hillslope (Figure 2a) behaves similarly for the same
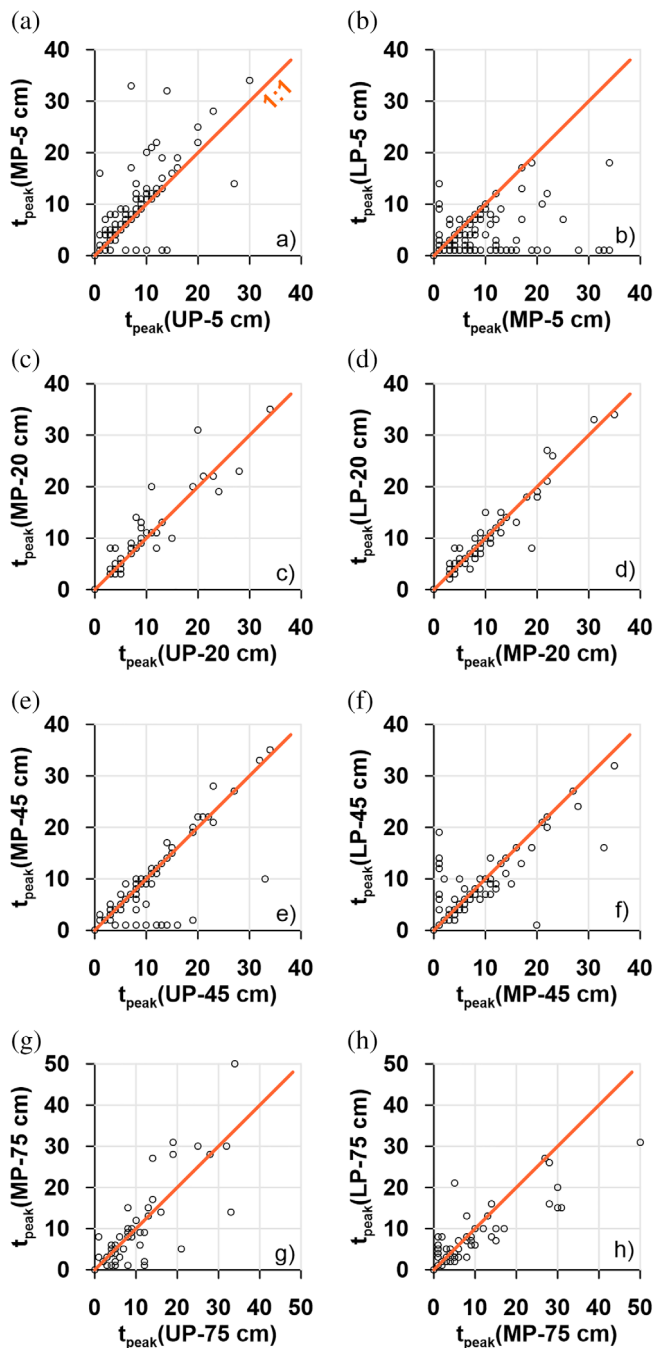
FIGURE 5 Relation of the response times in hours (t_{peak}) to the peak value of soil moisture during rainfall events between contiguous sampling positions (UP, MP, and LP sites) at a depth of 5 cm (a and b), 20 cm (c and d), 45 cm (e and f), and 75 cm (g and h). The orange line in each subplot represents the 1:1 ratio

reason, reflecting a fast hydraulic dynamic in the soil system. The combination of these effects in turn result in a rapid mobilization of water during precipitation events, explaining the flashy response of soil moisture in the Ah horizon.

Deeper in the subsurface (from 10–15 cm to 30–35 cm depth), the sustained near saturated conditions year-round (black lines in Figure 3b–d) indicate a perched water layer. These findings are in line

with those reported for organic rich soils in the Scottish highlands (Tetzlaff et al., 2014). The formation of this layer likely results from the abrupt vertical K_{sat} reduction in this soil layer compared to the overlying rooted layer (Table 2), caused by the lower density of fine roots (Bonell, Cassells, & Gilmour, 1983). Moreover, the high moisture (soil water storage) likely results from the high organic matter and clay content of the andic horizon (Table 1), to which water molecules can be easily bound (Yang et al., 2014).

The underlying transition layer (from 30–35 cm to 40–55 cm depth) also maintained a high moisture content throughout the year due to the high content of organic matter and clay of the Ah horizon (Table 1), but at a lower level than the perched layer above (brown lines in Figure 3b–d). The available pore space was quickly recharged during precipitation events, leading to a fast soil moisture response as in the rooted layer. This response likely results from the exponential soil moisture-matric potential relation of the soils' organic horizon (Figure 2a) that allows incoming water to fill rapidly the available pore space in the soil matrix (Hasegawa & Eguchi, 2002; Torres et al., 1998). This effect is likely due to the precipitation intensity (<2 mm hr^{-1}), which is generally lower than the vertical K_{sat} of the organic soil horizons (Table 2), thus enhancing the transmissivity of hydraulic potentials during rainfall events. A noteworthy difference in this layer was observed between the UP and MP sites. This difference reflects possibly the higher content of mineral and coarse particles at the MP site, as observed in the field and indicated by the higher BD and a lower soil moisture content at saturation compared to the UP site (Table 2). This factor is also likely responsible for the observed lower moisture (water storage) at the MP site in comparison to the UP site (brown lines in Figure 3b,c, respectively).

The fast soil moisture dynamics in the underlying mineral layer (from 40–55 cm to 70–80 cm depth) indicate that this layer is quickly recharged by water from the Ah horizon during rainfall events (orange lines in Figure 3b,d). This effect is likely explained by the steep gradient of the water retention curve of the mineral horizon at high matric potentials (Figure 2b), similar to that of the organic horizon. This soil moisture-matric potential relation facilitates a rapid transfer of hydraulic potentials through the mineral horizon, which in turn causes a fast soil moisture response to precipitation inputs of water that infiltrated through the Ah horizon during rainfall events (Torres et al., 1998). The observed soil moisture variations, however, occurred at lower water content than those within the Ah horizon. This lower moisture content reflects the lower clay fraction and organic matter content in the mineral horizon, which decreased to about a third to fourth of those in the Ah horizon (Table 1).

As lateral flow is more prone to be activated under high moisture conditions, hypothetically, if upper hillslope portions would contribute substantial moisture downslope via lateral subsurface flow, a delay in the response times in downhill positions with respect to uphill positions during rainfall events would be observed. However, the strong synchronization of response times to the peak values of soil moisture and groundwater level along the entire experimental hillslope (i.e., most scatter points in Figures 4 and 5 plot near the 1:1 ratio) indicates that during rainfall events a dominance of vertical flow paths of
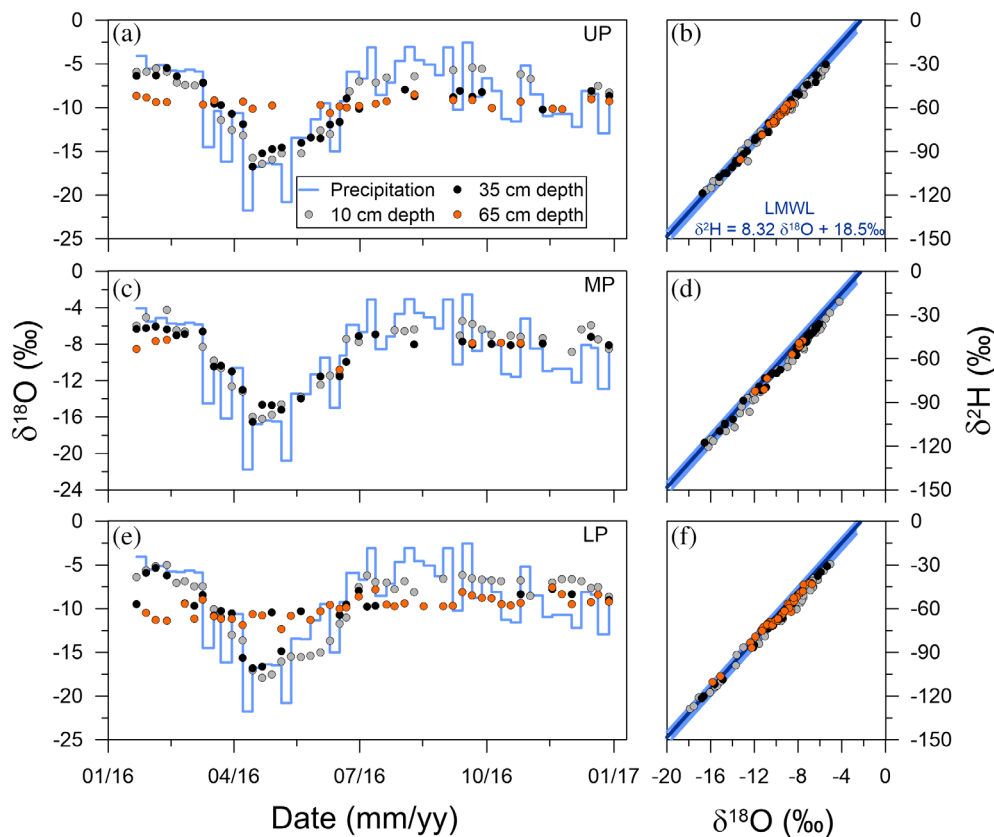
FIGURE 6 Temporal variability of the weekly $\delta^{18}O$ isotopic composition of precipitation (light blue line) and soil water (a, c, and e) and the δ^2H-$\delta^{18}O$ relation in precipitation (local meteoric water line, LMWL) and soil water (b, d, and f) at the upper (UP), middle (MP), and lower (LP) positions along the experimental hillslope during the period January 2016–January 2017. The dark blue lines and the light blue shaded areas in subplots (b), (d), and (f) represent the LMWL and the range of the isotopic variation in precipitation, respectively

water persists. These findings are further supported by soil moisture and groundwater level observations during dry periods (e.g., September–October 2017; Figure 3). During these periods, not surprisingly, groundwater levels showed a very sharp and steady reduction at faster rates than soil moisture observations did. These findings indicate that the aforementioned hydrological dynamics, enabled by the properties of the Andosol soils, facilitate the vertical percolation of water throughout the year despite the perched layer formed below the rooted zone. Nevertheless, it is worth noting the likely occurrence of lateral subsurface flow in the thin transition zones (<few centimeters) between soil layers with marked differences in hydraulic conductivity (e.g., the transitions between the rooted and perched layers, and the C horizon and the compact bedrock), which we observed during field work, but whose hydrological dynamics could not be captured through our monitoring system.

5.2 | Tracer mixing and soil water ages

Precipitation affected greatly the mixing of water in the rooted layer, as evidenced by the little attenuation of the stable isotopic composition of soils water (grey dots in Figure 6). These observations further indicate that water molecules residing in this soil layer are rapidly replaced by incoming water during precipitation events (Mosquera, Célleri, et al., 2016), thus explaining the short MTT of water in this soil layer (about 2 weeks at all sampling sites; Figure 7a and Table 3).

Past research suggested that a perched water layer in the subsurface implies that vertical percolation in a soil–regolith–bedrock continuum is substantially reduced, while lateral subsurface flow in the overlaying layer is favored (Dykes & Thornes, 2000; Hardie, Doyle, Cotching, & Lisson, 2012). Thus, solely based on soil moisture observations, we expect that the time water resided in this soil layer was much longer than the one in the fast reacting rooted layer above. Surprisingly, however, results from the SWI data and MTT analyses indicate that the isotopic composition of the water stored in the perched layer is highly influenced by the isotopic composition of precipitation (black dots in Figure 6a,c,e) and resides in the subsurface for a short time (about a month at all sampling sites; Figure 7b and Table 3). Similar MTTs have been previously reported for Andosols in a nearby Páramo catchment at 25 cm depth (35 days; Lazo et al., 2019; Mosquera, Célleri, et al., 2016) and in a temperate humid forest catchment in central eastern Mexico at 30 cm depth (36 ± 10 days; Muñoz-Villers & McDonnell, 2012).

The soil water MTTs at this soil horizon increased with depth at each hillslope position, but were consistently similar at each depth among all sampling sites, similar to the vertical aging of water in a tropical forest catchment dominated by Andosol soils (Muñoz-Villers & McDonnell, 2012). The sole vertical aging of soil water indicates that water from upslope areas does not significantly contribute to lower hillslope positions, and thus, that vertical flow paths of water are dominant (Asano et al., 2002; McGuire & McDonnell, 2010; Muñoz-Villers & McDonnell, 2012). These findings are concomitant with the aforementioned fast transfer of hydraulic potentials across the entire
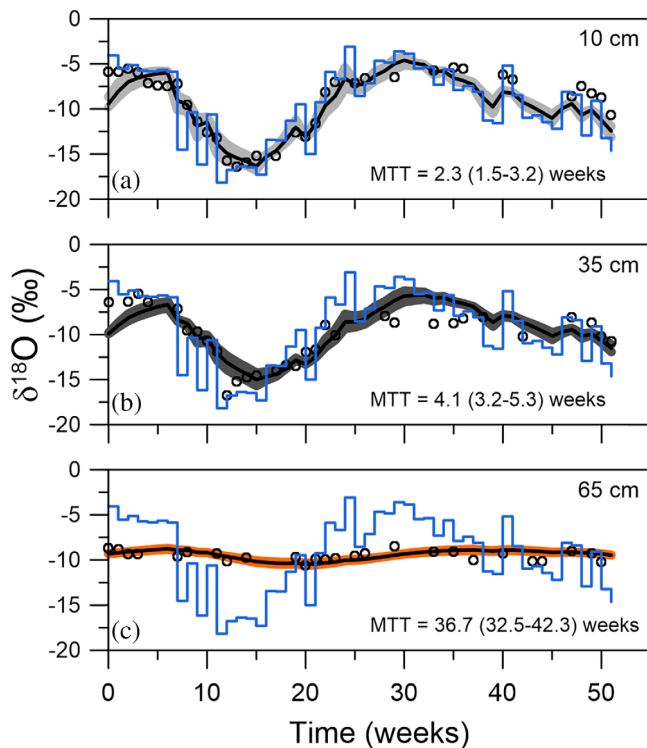
FIGURE 7 Observed and simulated soil water δ¹⁸O isotopic composition at (a) 10 cm, (b) 35 cm, and (c) 65 cm depths at the upper position (UP) of the experimental hillslope. The open circles represent the observed isotopic composition in soil water; the blue lines represent the precipitation isotopic composition; the black lines represent the best simulated isotopic composition in soil water according to the KGE objective function; and the shaded areas represent the 5–95% confidence limits of the simulated soil water MTTs presented in parenthesis (Table 3). KGE, Kling–Gupta efficiency; MTT, mean transit time

organic (andic) horizon of the hillslope soils, being the result from the fast movement of water through the porous soil matrix. Moreover, the transport and mixing of water throughout the whole Ah horizon suggests that the perched layer is hydrologically active, balancing out gains and losses of moisture during rainfall events. This behavior can be explained by the combined effect of two characteristics of the soil. On the one hand, the high content of organic matter and clay of the soil that allow water molecules to be bound to the large surface area of the soil particles. On the other hand, the rapid transport of water through the soil that enables the replacement of stored moisture by "new" water molecules during rainstorms.

Despite the fast transfer of hydraulic potentials from the organic horizon to the mineral horizon during rainfall events, soil water stored within the mineral layer was less influenced by the isotopic composition of incoming precipitation and had longer MTTs (2.8–8.5 months; Table 3) than in the organic horizon. Similar SWI signals for the mineral layer of Andosols have been reported in a nearby Páramo catchment (Lazo et al., 2019; Mosquera, Célleri, et al., 2016) and in a tropical forest catchment in Veracruz, Mexico (Muñoz-Villers & McDonnell, 2012). Even though the dominance of rapid infiltration of incoming precipitation across the Ah horizon toward the mineral layer is consistent with the relatively short MTT observed at the LP site (2.8 months), this mechanism cannot explain the longer MTT at the UP site (8.5 months). A potential explanation for the long MTT at the latter could be the reduced lateral inflow at upper hillslope positions within the mineral layer due to smaller upslope contributing area in relation to the downslope sites. This effect could result in an overall lower exchange of the water stored at upslope sampling positions and hence explain (a) the generally longer MTTs of soil water in the mineral layer in relation to the organic horizon and (b) the longer MTT and slower response times to the peak values of soil moisture during rainfall events (Figure 5g,h) at

TABLE 3 Summary statistics of the δ¹⁸O isotopic composition of precipitation (QP1) and soil water and the soil water mean transit times (MTTs) at the upper (UP), middle (MP), and lower (LP) positions along the experimental hillslope

| Sample type | Sampling station | Altitude (m a.s.l.) | Depth (cm) | δ¹⁸O (‰) | | | | | MTT (days) |
				n	Mean	SE	Max	Min	
Precipitation	QP1	3,955	n/a[a]	58	−10.0	0.6	−2.5	−21.8	n/a[a]
Soil water	UP	4,006	10	41	−9.7	0.5	−5.4	−16.4	15.8 (10.3–22.2)
			35	38	−10.7	0.5	−5.5	−16.7	29.0 (22.3–37.3)
			65	32	−9.9	0.2	−8.5	−13.3	256.8 (227.5–296.2)
	MP	3,958	10	47	−9.3	0.5	−4.2	−16.2	15.2 (9.6–22.2)
			35	47	−9.6	0.4	−6.1	−16.5	25.5 (19.0–33.2)
			65	13	−9.9	0.5	−7.6	−12.3	n/p[b]
	LP	3,913	10	53	−9.7	0.5	−5.0	−17.9	11.8 (6.9–18.9)
			35	27	−10.2	0.6	−5.3	−16.8	24.5 (17.4–32.8)
			65	53	−9.9	0.2	−6.7	−15.8	83.8 (72.2–99.0)

Note: MTT values in parenthesis represent the 5–95% confidence limits of the simulated soil water MTTs.
Abbreviations: Max, maximum; Min, Minimum; *n*, number of samples; SE, standard error.
[a]Not applicable.
[b]Not possible to estimate the soil water mean transit time since there were not enough samples to run the model due to malfunctioning of the wick sampler during the study period.
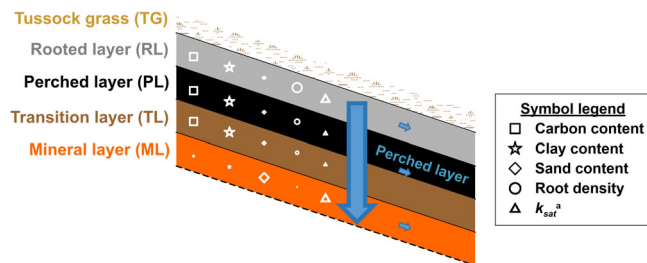
FIGURE 8 "A wet, layered sloping sponge". Conceptual model of the subsurface hydrological system of the experimental hillslope underlain by volcanic ash soils (Andosols) located in the headwaters of the Quinuas Ecohydrological Observatory. The size of the blue arrows represents the relative importance of vertical and lateral flow paths of water at different soil layers. The relative size of the white symbols indicates differences in the magnitude of the soil properties at each of the soil layers (values in Tables 1 and 2). [a]K_{sat}, saturated hydraulic conductivity in the vertical direction

the UP site in comparison to the LP site. The activation of lateral flow paths in this soil layer is likely favored by the compacted underlying geology observed during the excavation of the soil pits.

5.3 | Volcanic ash soils as wet, layered sloping sponges?

The hydraulic properties of household cellulose sponges were experimentally examined and compared to soils with different characteristics by Richardson and Siccama (2000) to investigate whether the forest hydrology analogy of soils behaving like "sponges" is a fair comparison from a soil physics point of view. Their findings suggested that sponges (O-Cel-O cellulose sponges, 3M) had similar water retention and release characteristics as soils rich in organic matter, that is, topsoil and peat. Our field observations and soil properties characterization suggest that the organic layer of the Andosol soils are able to store large amounts of water and to rapidly transfer hydraulic potentials in a similar manner to the cellulose sponges. Thus, our findings provide novel field evidence to support the experimental observations reported by Richardson and Siccama (2000) and indicate that volcanic ash soils (rich in organic matter and clay) resemble a "sponge-like" hydrological behavior.

Our natural soil system, however, presents some particularities with respect to the "ideal" sponge behavior. Even though the organic matter and clay content of the organic horizon of the soils are homogenous along the experimental hillslope, K_{sat} decreased consistently with depth at all positions. These factors allow incoming water to rapidly fill and empty the porous matrix of the unsaturated layers with high K_{sat} (the rooted layer), but tend to promote a sustained storage of high amounts of water and to transport it steadily to deeper soil layers with low K_{sat} (the perched layer). The latter phenomenon is also possible at our study site given that precipitation is distributed fairly even throughout the year, with generally low intensity compared to the K_{sat} of the soil, thus maintaining near saturation conditions in the organic layers below the highly conductive root zone. This results in

the formation of a "layered sponge" system, in which a fast-conducting organic layer underlain by a lower conductivity layer helps conserve high soil moisture near saturated conditions year-round in the latter (Figure 8). This situation, in turn, provides water for vegetation throughout the year, creating a positive hydrological service. Even though topography has been found an important factor controlling subsurface flow processes (Bachmair & Weiler, 2012; Famiglietti, Rudnicki, & Rodell, 1998), our findings illustrate clearly the dominance of vertical flow paths independent of the position along the steep hillslope. Thus, it is not unlikely that the conceptual system representation can be used to mimic the hydrological functioning of hillslopes dominated by volcanic ash soils with similar to lower slope gradients.

6 | CONCLUSIONS

The experimental evaluation of water transport and tracer mixing helped to conceptualize the subsurface hydrological behavior of a steep experimental hillslope underlain by volcanic ash soils (Andosols). Findings reveal that the behavior resembles that of a "layered sponge" in which vertical flow paths are dominant. That is, on the one hand, the formation of a perched water layer that maintains high moisture near saturated conditions year-round due to the presence of a low conductivity layer below a layer with a higher conductivity. On the other hand, a fast vertical transport of water due to the rapid transfer of hydraulic potentials along the entire soil profile facilitating water mobilization through the porous soil matrix. Despite the dominance of vertical flow paths, lateral flow likely develops during high intensity rainstorm events above hydraulically restrictive layers (e.g., the perched layer) due to the steep slope of the hillslope. Given that the "sponge-like" hydrological behavior of these soils largely depends on their high organic matter and clay content, the rapid breakdown of the soil organic-mineral components due to changes in land use and climate could cause severe changes in the hydrological services provided by ecosystems in which these soils dominate. The findings of this study provide crucial information that can be used to improve the representation of the physical processes in hydrological models, which in turn will lead to a better management of the soil and water resources in these ecosystems.

DATA AVAILABILITY STATEMENT

ORCID

Giovanny M. Mosquera https://orcid.org/0000-0002-4764-4685

REFERENCES

Anderson, A. E., Weiler, M., Alila, Y., & Hudson, R. O. (2009). Subsurface flow velocities in a hillslope with lateral preferential flow. *Water Resources Research*, 45(11), W11407. https://doi.org/10.1029/2008WR007121

Asano, Y., Uchida, T., & Ohte, N. (2002). Residence times and flow paths of water in steep unchannelled catchments, Tanakami, Japan. *Journal of Hydrology*, 261(1–4), 173–192. https://doi.org/10.1016/S0022-1694(02)00005-7

Bachmair, S., & Weiler, M. (2012). Hillslope characteristics as controls of subsurface flow variability. *Hydrology and Earth System Sciences*, 16(10), 3699–3715. https://doi.org/10.5194/hess-16-3699-2012

Benettin, P., Soulsby, C., Birkel, C., Tetzlaff, D., Botter, G., & Rinaldo, A. (2017). Using SAS functions and high resolution isotope data to unravel travel time distributions in headwater catchments. *Water Resources Research*, 53, 1864–1878. https://doi.org/10.1002/2016WR020117

Blume, T., Zehe, E., & Bronstert, A. (2009). Use of soil moisture dynamics and patterns at different spatio-temporal scales for the investigation of subsurface flow processes. *Hydrological Processes*, 13(7), 1215–1233.

Boelter, D. H. (1969). Physical properties of peats as related to degree of decomposition. *Soil Science Society of America Proceedings*, 33, 606–609.

Bonell, M., Cassells, D. S., & Gilmour, D. A. (1983). Vertical soil water movement in a tropical rainforest catchment in Northeast Queensland. *Earth Surface Processes and Landforms*, 8(3), 253–272. https://doi.org/10.1002/esp.3290080307

Buytaert, W., Célleri, R., De Bièvre, B., Cisneros, F., Wyseure, G., Deckers, J., & Hofstede, R. (2006). Human impact on the hydrology of the Andean páramos. *Earth-Science Reviews*, 79(1–2), 53–72. https://doi.org/10.1016/j.earscirev.2006.06.002

Buytaert, W., Deckers, J., & Wyseure, G. (2006). Description and classification of nonallophanic Andosols in south Ecuadorian alpine grasslands (páramo). *Geomorphology*, 73(3–4), 207–221. https://doi.org/10.1016/j.geomorph.2005.06.012

Carrillo-Rojas, G., Silva, B., Rollenbeck, R., Célleri, R., & Bendix, J. (2019). The breathing of the Andean highlands: Net ecosystem exchange and evapotranspiration over the páramo of southern Ecuador. *Agricultural and Forest Meteorology*, 265, 30–47. https://doi.org/10.1016/J.AGRFORMET.2018.11.006

Craig, H. (1961). Standard for reporting concentrations of deuterium and Oxygen-18 in natural waters. *Science (New York, N.Y.)*, 133(3467), 1833–1834. https://doi.org/10.1126/science.133.3467.1833

Dec, D., Zúniga, F., Thiers, O., Paulino, L., Valle, S., Villagra, V., … Dörner, J. (2017). Water and temperature dynamics of Aquands under different uses in southern Chile. *Journal of Soil Science and Plant Nutrition*, 17(1), 141–154. https://doi.org/10.4067/S0718-95162017005000011

Dunkerley, D. (2008). Identifying individual rain events from pluviograph records: A review with analysis of data from an Australian dryland site. *Hydrological Processes*, 22(26), 5024–5036.

Dykes, A. P., & Thornes, J. B. (2000). Hillslope hydrology in tropical rainforest steeplands in Brunei. *Hydrological Processes*, 14(2), 215–235.

https://doi.org/10.1002/(SICI)1099-1085(20000215)14:2<215::AID-HYP921>3.0.CO;2-P

Eguchi, S., & Hasegawa, S. (2008). Determination and characterization of preferential water flow in unsaturated subsoil of Andisol. *Soil Science Society of America Journal*, 72(2), 320–330. https://doi.org/10.2136/sssaj2007.0042

Esquivel-Hernández, G., Mosquera, G. M., Sánchez-Murillo, R., Quesada-Román, A., Birkel, C., Crespo, P., … Boll, J. (2019). Moisture transport and seasonal variations in the stable isotopic composition of rainfall in Central American and Andean Páramo during El Niño conditions (2015-2016). *Hydrological Processes*, 33(13), 1802–1817. https://doi.org/10.1002/hyp.13438

Famiglietti, J. S., Rudnicki, J. W., & Rodell, M. (1998). Variability in surface moisture content along a hillslope transect: Rattlesnake Hill, Texas. *Journal of Hydrology*, 210(1–4), 259–281. https://doi.org/10.1016/S0022-1694(98)00187-5

Fan, Y., Clark, M., Lawrence, D. M., Swenson, S., Band, L. E., Brantley, S. L., … Yamazaki, D. (2019). Hillslope hydrology in global change research and earth system modeling. *Water Resources Research*, 55(2), 1737–1772. https://doi.org/10.1029/2018WR023903

FAO (2002). In L. P. van Reeuwijk (Ed.), *Procedures for soil analysis*. Roma, Italy: Author.

FAO. (2006). *Guidelines for soil description*. Rome, Italy: FAO-ISRIC Press.

Fontes, J. C., Gonçalves, M. C., & Pereira, L. S. (2004). Andosols of Terceira, Azores: Measurement and significance of soil hydraulic properties. *CATENA*, 56(1–3), 145–154. https://doi.org/10.1016/J.CATENA.2003.10.008

Guo, L., & Gifford, R. M. (2002). Soil carbon stocks and land use change: A meta analysis. *Global Change Biology*, 8(4), 345–360. https://doi.org/10.1046/j.1354-1013.2002.00486.x

Gupta, H. V., Kling, H., Yilmaz, K. K., & Martinez, G. F. (2009). Decomposition of the mean squared error and NSE performance criteria: Implications for improving hydrological modelling. *Journal of Hydrology*, 377(1–2), 80–91. https://doi.org/10.1016/j.jhydrol.2009.08.003

Hardie, M. A., Doyle, R. B., Cotching, W. E., & Lisson, S. (2012). Subsurface lateral flow in texture-contrast (duplex) soils and catchments with shallow bedrock. *Applied and Environmental Soil Science*, 2012, 1–10. https://doi.org/10.1155/2012/861358

Harman, C. J. (2015). Time-variable transit time distributions and transport: Theory and application to storage-dependent transport of chloride in a watershed. *Water Resources Research*, 51(1), 1–30. https://doi.org/10.1002/2014WR015707

Hasegawa, S., & Eguchi, S. (2002). Soil water conditions and flow characteristics in the subsoil of a volcanic ash soil: Findings from field monitoring from 1997 to 1999. *Soil Science and Plant Nutrition*, 48(2), 227–236. https://doi.org/10.1080/00380768.2002.10409195

Hasegawa, S., & Sakayori, T. (2000). Monitoring of matrix flow and bypass flow through the subsoil in a volcanic ash soil. *Soil Science and Plant Nutrition*, 46(3), 661–671. https://doi.org/10.1080/00380768.2000.10409131

Hrachowitz, M., Benettin, P., van Breukelen, B. M., Fovet, O., Howden, N. J. K., Ruiz, L., … Wade, A. J. (2016). Transit times-the link between hydrology and water quality at the catchment scale. *Wiley Interdisciplinary Reviews: Water*, 3(5), 629–657. https://doi.org/10.1002/wat2.1155

van Huijgevoort, M. H. J., Tetzlaff, D., Sutanudjaja, E. H., & Soulsby, C. (2016). Using high resolution tracer data to constrain water storage, flux and age estimates in a spatially distributed rainfall-runoff model. *Hydrological Processes*, 30(25), 4761–4778. https://doi.org/10.1002/hyp.10902

ISO 11277. (2009). Soil quality—Determination of particle size distribution in mineral soil material—Method by sieving and sedimentation, Reference Number ISO 11277:2009(E). Geneva, Switzerland.

IUSS Working Group WRB. (2015). World Reference Base for Soil Resources 2014, update 2015. International soil classification system for

naming soils and creating legends for soil maps. World Soil Resources Reports No. 106. FAO, Rome.

Kim, S., & Jung, S. (2014). Estimation of mean water transit time on a steep hillslope in South Korea using soil moisture measurements and deuterium excess. *Hydrological Processes*, 28(4), 1844–1857. https://doi.org/10.1002/hyp.9722

Kirchner, J. W. (2016). Aggregation in environmental systems—Part 1: Seasonal tracer cycles quantify young water fractions, but not mean transit times, in spatially heterogeneous catchments. *Hydrology and Earth System Sciences*, 20(1), 279–297. https://doi.org/10.5194/hess-20-279-2016

Lazo, P. X., Mosquera, G. M., McDonnell, J. J., & Crespo, P. (2019). The role of vegetation, soils, and precipitation on water storage and hydrological services in Andean Páramo catchments. *Journal of Hydrology*, 572, 805–819. https://doi.org/10.1016/J.JHYDROL.2019.03.050

Letts, M. G., Roulet, N. T., Comer, N. T., Skarupa, M. R., & Verseghy, D. L. (2000). Parametrization of peatland hydraulic properties for the Canadian land surface scheme. *Atmosphere-Ocean*, 38(1), 141–160. https://doi.org/10.1080/07055900.2000.9649643

Lin, H. (2010). Earth's critical zone and hydropedology: Concepts, characteristics, and advances. *Hydrology and Earth System Sciences*, 14, 25–45.

Lozano-Parra, J., van Schaik, N. L. M. B., Schnabel, S., & Gómez-gutiérrez, Á. (2015). Soil moisture dynamics at high temporal resolution in a semiarid Mediterranean watershed with scattered tree cover. *Hydrological Processes*, 30, 8. https://doi.org/10.1002/hyp.10694

Maloszewski, P., & Zuber, A. (1996). Lumped parameter models for the interpretation of environmental tracer data. In *Manual on Mathematical Models in Isotope Hydrogeology*. TECDOC-910.

McDaniel, P. A., Lowe, D. J., Arnalds, O., & Ping, C.-L. (2012). Andisols. In P. M. Huang, Y. Li, & M. E. Summer (Eds.), *Handbook of soil sciences: Properties and processes* (pp. 29–48). Boca Raton, FL: CRC Press.

McDonnell, J., Owens, I., & Stewart, M. (1991). A case study of shallow flow paths in a steep zero-order basin. *Journal of the American Water Resources Association*, 27(4), 679–685. https://doi.org/10.1111/j.1752-1688.1991.tb01469.x

McGuire, K. J., & McDonnell, J. J. (2006). A review and evaluation of catchment transit time modeling. *Journal of Hydrology*, 330(3–4), 543–563. https://doi.org/10.1016/j.jhydrol.2006.04.020

McGuire, K. J., & McDonnell, J. J. (2010). Hydrological connectivity of hillslopes and streams: Characteristic time scales and nonlinearities. *Water Resources Research*, 46(10), W10543. https://doi.org/10.1029/2010WR009341

Mertens, J., & Vanderborght, J. (2007). Numerical analysis of passive capillary wick samplers prior to field installation. *Soil Science Society of America Journal*, 1991, 35–42. https://doi.org/10.2136/sssaj2006.0106

Minnesota Board of Water & Soil Resources. (2013). *Hydrologic monitoring of wetlands*. St Paul, MN: Minnesota Board of Water & Soil Resources

Montenegro-Díaz, P., Ochoa-Sánchez, A., & Célleri, R. (2019). Impact of tussock grasses removal on soil water content dynamics of a tropical mountain hillslope. *Ecohydrology*, 12(8), e2146. https://doi.org/10.1002/eco.2146

Mook, W. G. (2000). Introduction: Theory, methods, review. In W. G. Mook (Ed.), *Environmental isotopes in the hydrological cycle: Principles and applications*. Paris, Vienna: IAEA and UNESCO.

Mosquera, G. M., Célleri, R., Lazo, P. X., Vaché, K. B., Perakis, S. S., & Crespo, P. (2016). Combined use of isotopic and hydrometric data to conceptualize ecohydrological processes in a high-elevation tropical ecosystem. *Hydrological Processes*, 30, 2930–2947. https://doi.org/10.1002/hyp.10927

Mosquera, G. M., Lazo, P. X., Célleri, R., Wilcox, B. P., & Crespo, P. (2015). Runoff from tropical alpine grasslands increases with areal extent of wetlands. *Catena*, 125, 120–128. https://doi.org/10.1016/j.catena.2014.10.010

Mosquera, G. M., Segura, C., Vaché, K. B., Windhorst, D., Breuer, L., & Crespo, P. (2016). Insights into the water mean transit time in a high-elevation tropical ecosystem. *Hydrology and Earth System Sciences*, 20(7), 2987–3004. https://doi.org/10.5194/hess-20-2987-2016

Muñoz-Villers, L. E., & McDonnell, J. J. (2012). Runoff generation in a steep, tropical montane cloud forest catchment on permeable volcanic substrate. *Water Resources Research*, 48(9), W09528. https://doi.org/10.1029/2011WR011316

Muñoz-Villers, L. E., Geissert, D. R., Holwerda, F., & Mcdonnell, J. J. (2016). Factors influencing stream baseflow transit times in tropical montane watersheds. *Hydrology and Earth System Sciences*, 20, 1621–1635. https://doi.org/10.5194/hess-20-1621-2016

Muñoz, P., Célleri, R., & Feyen, J. (2016). Effect of the resolution of tipping-bucket rain gauge and calculation method on rainfall intensities in an Andean mountain gradient. *Water*, 8(11), 534. https://doi.org/10.3390/w8110534

Muñoz, P., Orellana-Alvear, J., Willems, P., & Célleri, R. (2018). Flash-flood forecasting in an Andean mountain catchment—Development of a step-wise methodology based on the random forest algorithm. *Water*, 10(11), 1519. https://doi.org/10.3390/w10111519

Neall, V. E. (2006). Volcanic soils. In W. Verheye (Ed.), *Land use and land cover, encyclopaedia of life support systems (EOLSS)* (pp. 1–24). Oxford, UK: EOLSS Publishers with UNESCO.

Ochoa-Sánchez, A., Crespo, P., Carrillo-Rojas, G., Marín, F., & Célleri, R. (2020). Unravelling evapotranspiration controls and components in tropical Andean tussock grasslands. *Hydrological Processes*. https://doi.org/10.1002/hyp.13716

Oosterbaan, R. J., & Nijland, H. J. (1994). Determining the saturated hydraulic conductivity. In H. Ritzema (Ed.), *Drainage principles and applications* (pp. 435–476). Wageningen, The Netherlands: International Institute for Land Reclamation and Improvement (ILRI).

Padrón, R. S., Wilcox, B. P., Crespo, P., & Célleri, R. (2015). Rainfall in the Andean Páramo: New insights from high-resolution monitoring in Southern Ecuador. *Journal of Hydrometeorology*, 16(3), 985–996. https://doi.org/10.1175/JHM-D-14-0135.1

Pesántez, J., Mosquera, G. M., Crespo, P., Breuer, L., & Windhorst, D. (2018). Effect of land cover and hydro-meteorological controls on soil water DOC concentrations in a high-elevation tropical environment. *Hydrological Processes*, 32(17), 2624–2635. https://doi.org/10.1002/hyp.13224

Picarro. (2010). *ChemCorrect TM-solving the problem of chemical contaminants in H_2O stable isotope research*. California: Author.

Richardson, A. D., & Siccama, T. G. (2000). Are soils like sponges? *Journal of the American Water Resources Association*, 36(4), 913–918. https://doi.org/10.1111/j.1752-1688.2000.tb04316.x

Rozanski K, Araguás-Araguás L, Gonfiantini R (1993). Isotopic Patterns in Modern Global Precipitation. In Swart P., Lohmann K., Mckenzie J., Savin S. (Eds). *Climate Change in Continental Isotopic Records*. Washington, D. C.: American Geophysical Union; 1–37.

Schwärzel, K., Renger, M., Sauerbrey, R., & Wessolek, G. (2002). Soil physical characteristics of peat soils. *Journal of Plant Nutrition and Soil Science*, 165(4), 479. https://doi.org/10.1002/1522-2624(200208)165:4<479::AID-JPLN479>3.0.CO;2-8

Soil Survey Staff. (1999). Soil taxonomy. USDA-NRCS, Agriculture Handbook No. 436.

Sprenger, M., Leistert, H., Gimbel, K., & Weiler, M. (2016). Illuminating hydrological processes at the soil-vegetation-atmosphere interface with water stable isotopes. *Reviews of Geophysics*, 54, 674–704. https://doi.org/10.1002/2015RG000515

Stewart, M. K., & McDonnell, J. J. (1991). Modeling base flow soil water residence times from deuterium concentrations. *Water Resources Research*, 27(10), 2681–2693. https://doi.org/10.1029/91WR01569

Stumpp, C., Maloszewski, P., Stichler, W., & Fank, J. (2009). Environmental isotope (δ18O) and hydrological data to assess water flow in unsaturated soils planted with different crops: Case study lysimeter station

"Wagna" (Austria). *Journal of Hydrology*, 369(1), 198–208. https://doi.org/10.1016/j.jhydrol.2009.02.047

Takahashi, T., & Shoji, S. (2002). Distribution and classification of volcanic ash soils. *Global Environmental Research*, 6, 83–97.

Tenelanda-Patiño, D., Crespo-Sánchez, P., & Mosquera-Rojas, G. (2018). Umbrales en la respuesta de humedad del suelo a condiciones meteorológicas en una ladera Altoandina. *MASKANA*, 9(2), 53–65. https://doi.org/10.18537/mskn.09.02.07

Tetzlaff, D., Birkel, C., Dick, J., Geris, J., & Soulsby, C. (2014). Storage dynamics in hydropedological units control hillslope connectivity, runoff generation, and the evolution of catchment transit time distributions. *Water Resources Research*, 50(2), 969–985. https://doi.org/10.1002/2013WR014147

Topp, G. C., & Zebchuk, W. (1979). The determination of soil-water desorption curves for soil cores. *Canadian Journal of Soil Science*, 59(1), 19–26. https://doi.org/10.4141/cjss79-003

Torres, R., Dietrich, W. E., Montgomery, D. R., Anderson, S. P., & Loague, K. (1998). Unsaturated zone processes and the hydrologic response of a steep, unchannelled catchment. *Water Resources Research*, 34(8), 1865–1879. https://doi.org/10.1029/98WR01140

Uchida, T., Kosugi, K., & Mizuyama, T. (1999). Runoff characteristics of pipeflow and effects of pipeflow on rainfall-runoff phenomena in a mountainous watershed. *Journal of Hydrology*, 222(1–4), 18–36. https://doi.org/10.1016/S0022-1694(99)00090-6

Vereecken, H., Huisman, J. A., Bogena, H., Vanderborght, J., Vrugt, J. A., & Hopmans, J. W. (2008). On the value of soil moisture measurements in vadose zone hydrology: A review. *Water Resources Research*, 44(4), W00D06. https://doi.org/10.1029/2008WR006829

Vereecken, H., Huisman, J. A., Hendricks Franssen, H. J., Brüggemann, N., Bogena, H. R., Kollet, S., … Vanderborght, J. (2015). Soil hydrology: Recent methodological advances, challenges, and perspectives. *Water Resources Research*, 51(4), 2616–2633. https://doi.org/10.1002/2014WR016852

White, J. W. C. (1989). *Stable hydrogen isotope ratios in plants: A review of current theory and some potential applications* (pp. 142–162). New York, NY: Springer. https://doi.org/10.1007/978-1-4612-3498-2_10

Windhorst, D., Kraft, P., Timbe, E., Frede, H.-G., & Breuer, L. (2014). Stable water isotope tracing through hydrological models for disentangling runoff generation processes at the hillslope scale. *Hydrology and Earth System Sciences*, 18(10), 4113–4127. https://doi.org/10.5194/hess-18-4113-2014

Yang, F., Zhang, G.-L., Yang, J.-L., Li, D.-C., Zhao, Y.-G., Liu, F., … Yang, F. (2014). Organic matter controls of soil water retention in an alpine grassland and its significance for hydrological processes. *Journal of Hydrology*, 519, 3086–3093. https://doi.org/10.1016/J.JHYDROL.2014.10.054

Zhu, Q., Nie, X., Zhou, X., Liao, K., & Li, H. (2014). Soil moisture response to rainfall at different topographic positions along a mixed land-use hillslope. *CATENA*, 119, 61–70. https://doi.org/10.1016/J.CATENA.2014.03.010